Supplementary material.

Table S1. Sentinel-1 image acquisition information.

Sensor	Platform	Orbit direction	Sensor mode	Polarization	Product	Period	Coverage	Data of image
Sentinel-1	1A	Descending	Interferometric Wide Swath (IW): 250 km with a moderate resolution of 5 m × 20 m	VV	Level-1 GRD (Ground Range Detected)	Pre-fire	District of Tahuamanu	May 16 and 21, 2020
				VH		Post-fire		October 1 and 6, 2020

Tabla S2. Sentinel-1 satellite image characteristics.

Parameter	Sentinel-1
Launch date	April 03, 2014 from S1-A April 22, 2016 from S1-B
Orbit type	SSO (sun-synchronous orbit) 12-day repeat cycle LTAN = 18:00 hrs.
Orbital altitude	693 kilometers
Sensors complement Spacecraft Mass Spacecraft Size Spacecraft Power	C-SAR (C-band synthetic aperture radar) 2,300 kg 3.4 m × 1.3 m × 1.3 m × 1.3 m 4.8 kW (EOL)
Downlink X-band data rate S-band TT&C	520 Mbit/s 64 kbit/s uplink 128 kbit/so 2 Mbit/s downlink
Science data storage Required data quality	1.4 Tbit (EOL) BER (bit error rate): < 10-9
Operational autonomy Prime contractor	8 days TAS-I (Thales Alenia Space-Italy)
Baseline Launcher	Soyuz (Kourou)

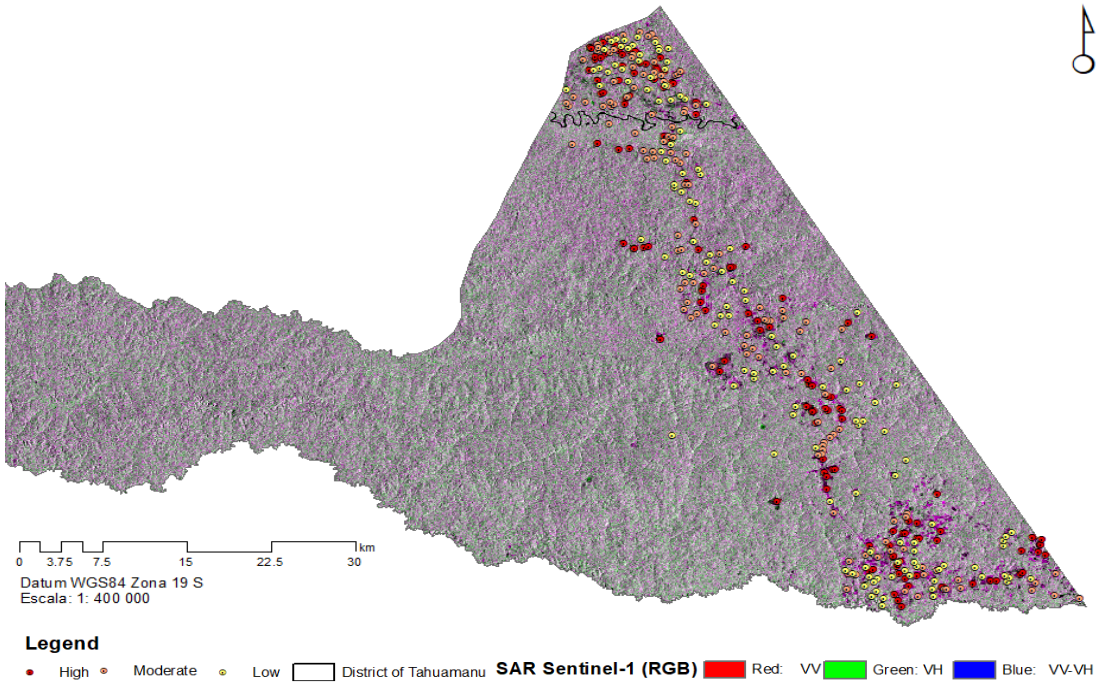

Figure S1. Distribution of samples to validate the severity of burns in the district of Tahuamanu, southeastern Peruvian Amazon.

Figure S2. Sentinel-1 C-band SAR images with VV polarization; pre and post fire 2020.

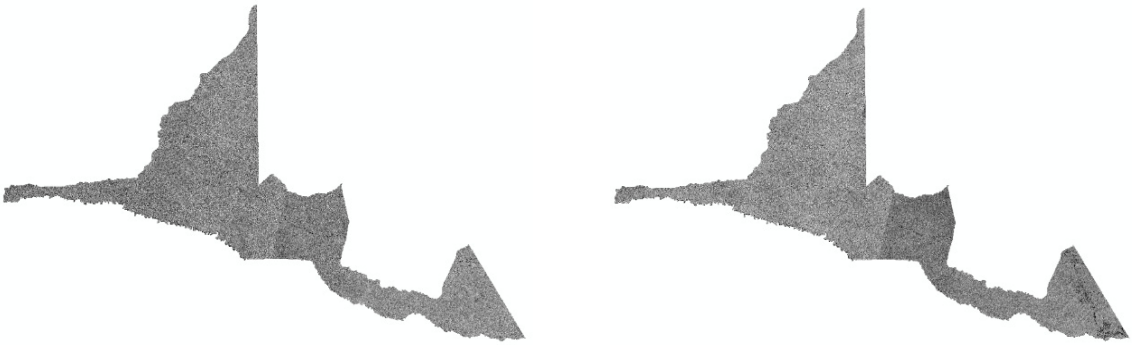

Figure S3. Sentinel-1 C-band SAR images with VH polarization; pre and post fire 2020.

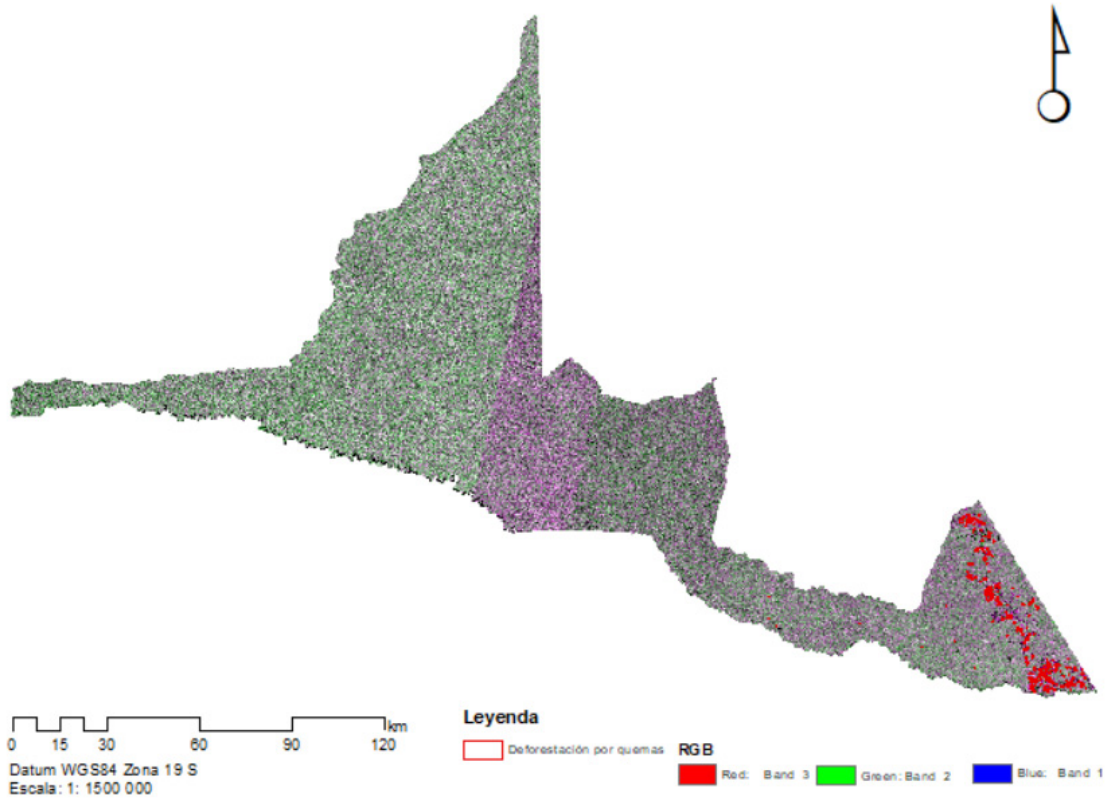

Figure S4. Determination of burned areas using absolute and relative values of pre- and post-fire 2020 VV_1 backscatter data; Equation 1 and 3.

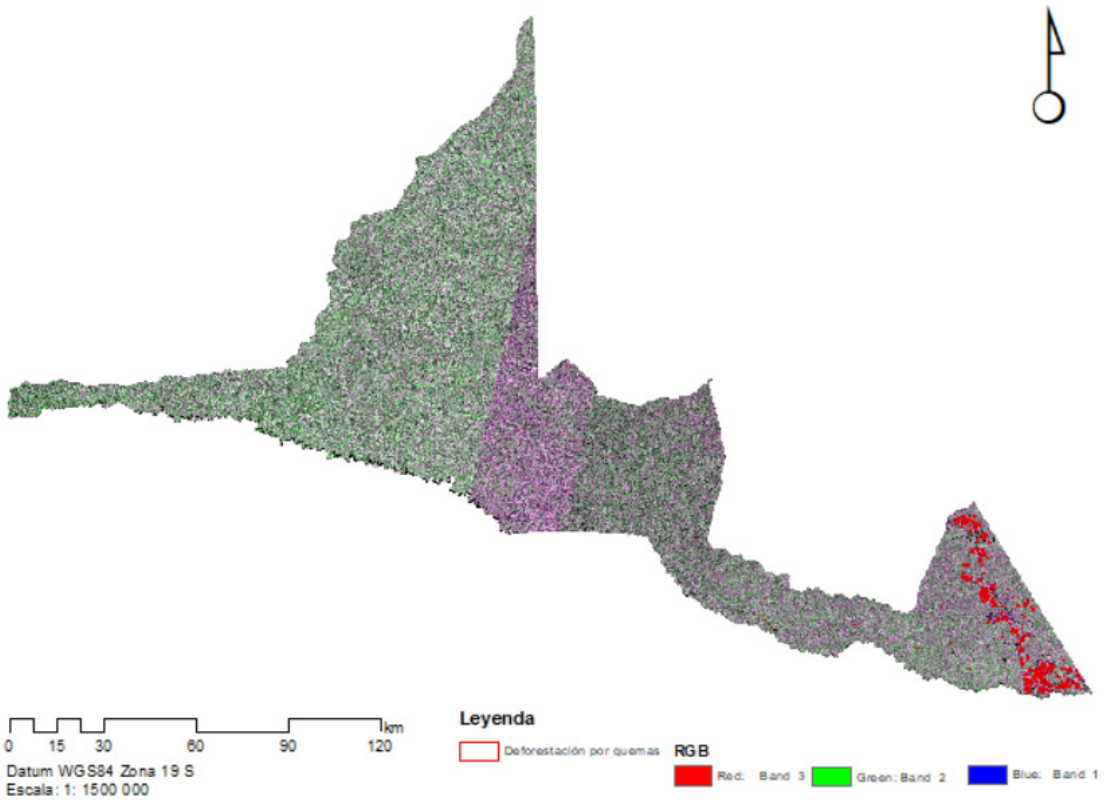

Figure S5. Determination of burned areas using absolute and relative values of pre- and post-fire 2020 VV_2 backscatter data; Equation 1 and 5.

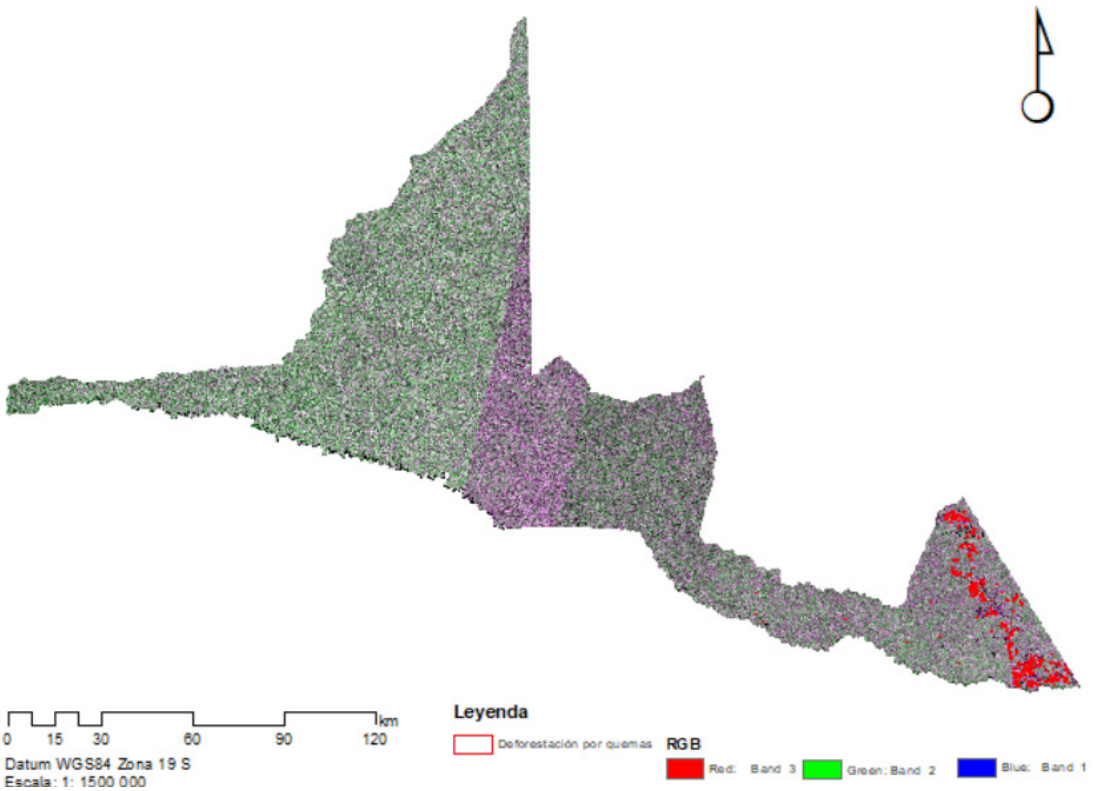

Figure S6. Determination of burned areas using absolute and relative values of pre- and post-fire 2020 VH_1 backscatter data; Equation 2 and 4.

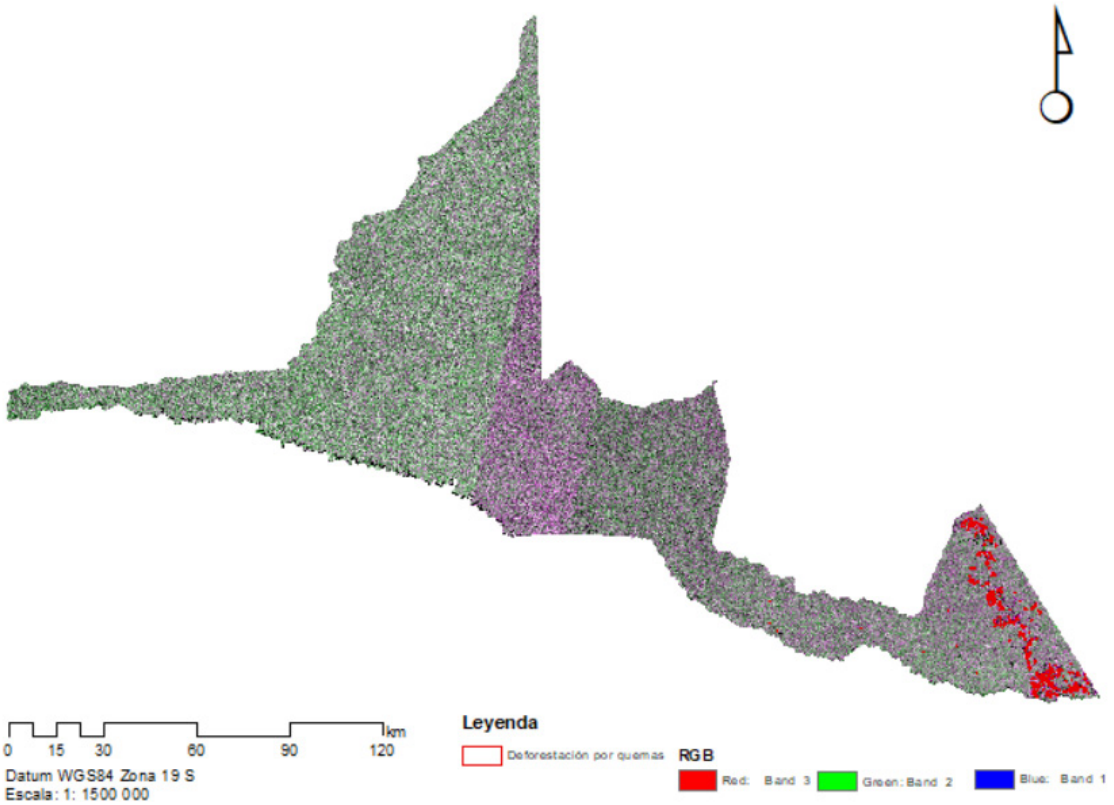

Figure S7. Determination of burned areas using absolute and relative values of pre- and post-fire 2020 VH_2 backscatter data; Equation 2 and 6.

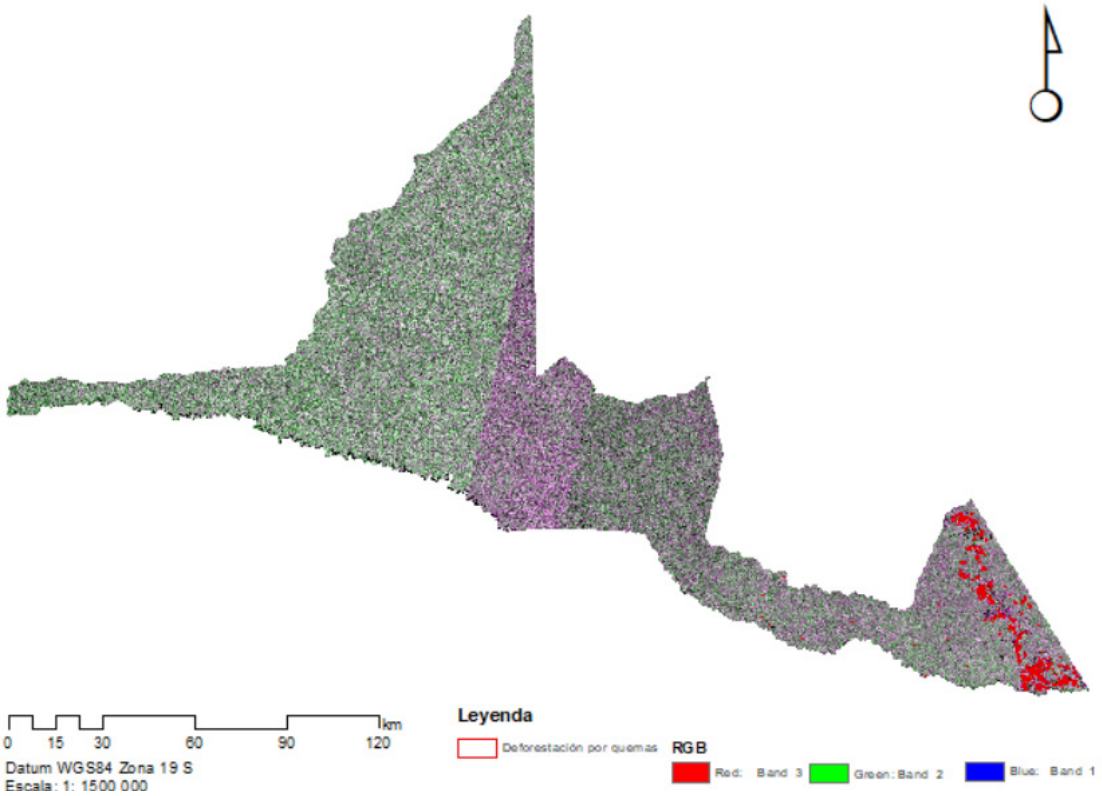

Figure S8. Determination of burned areas through Burn Ratio (RBR) by RADAR Forest Degradation Index (RDFI) from pre- and post-fire 2020 VV and VH backscatter data; Equation 8 and 9.

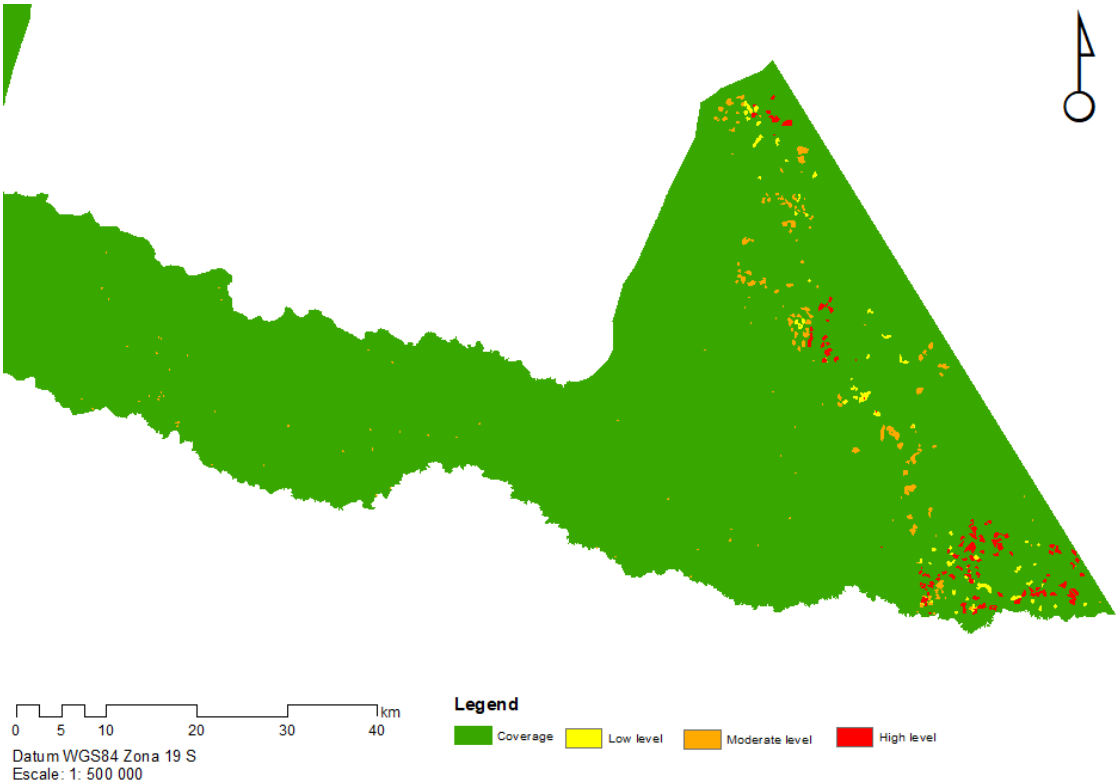

Figure S9. Burn severity using absolute, relative values from VV_1 pre- and post-fire 2020 backscatter data; Equation 1 and 3.

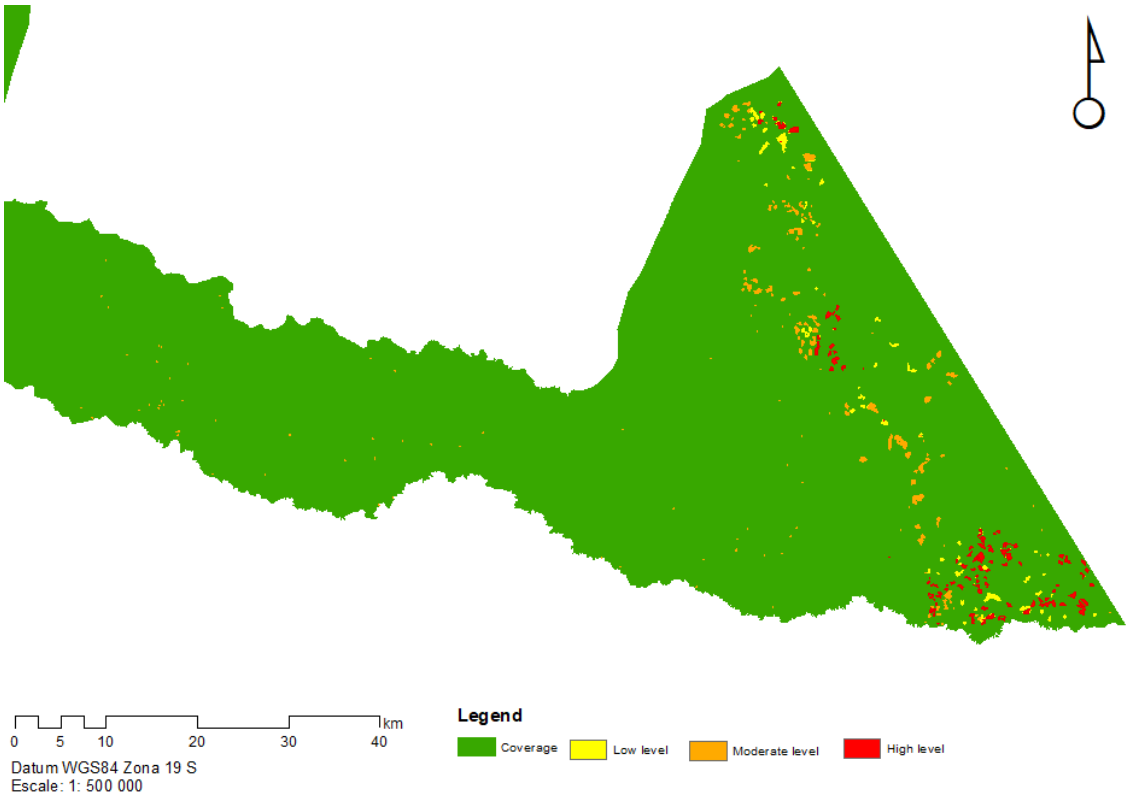

Figure S10. Burn severity using absolute, relative values from VV_2 pre- and post-fire 2020 backscatter data; Equation 1 and 5.

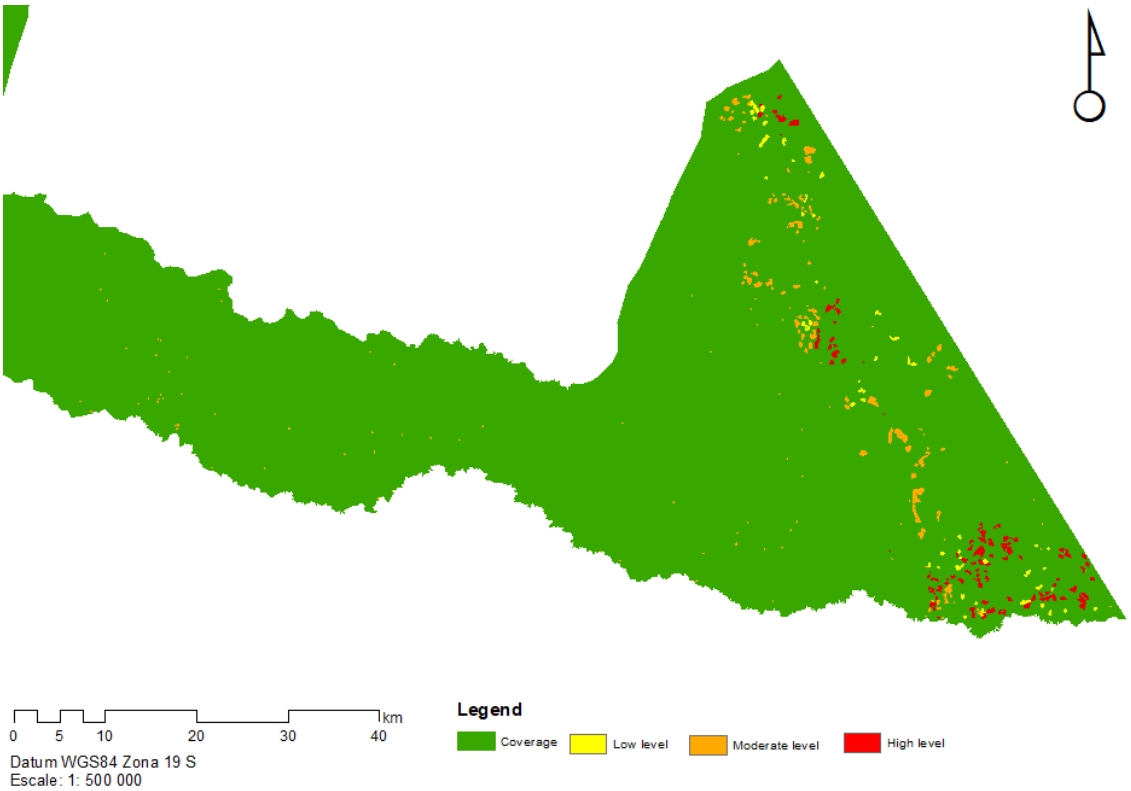

Figure S11. Burn severity using absolute, relative values from VH_1 pre- and post-fire 2020 backscatter data; Equation 2 and 4.

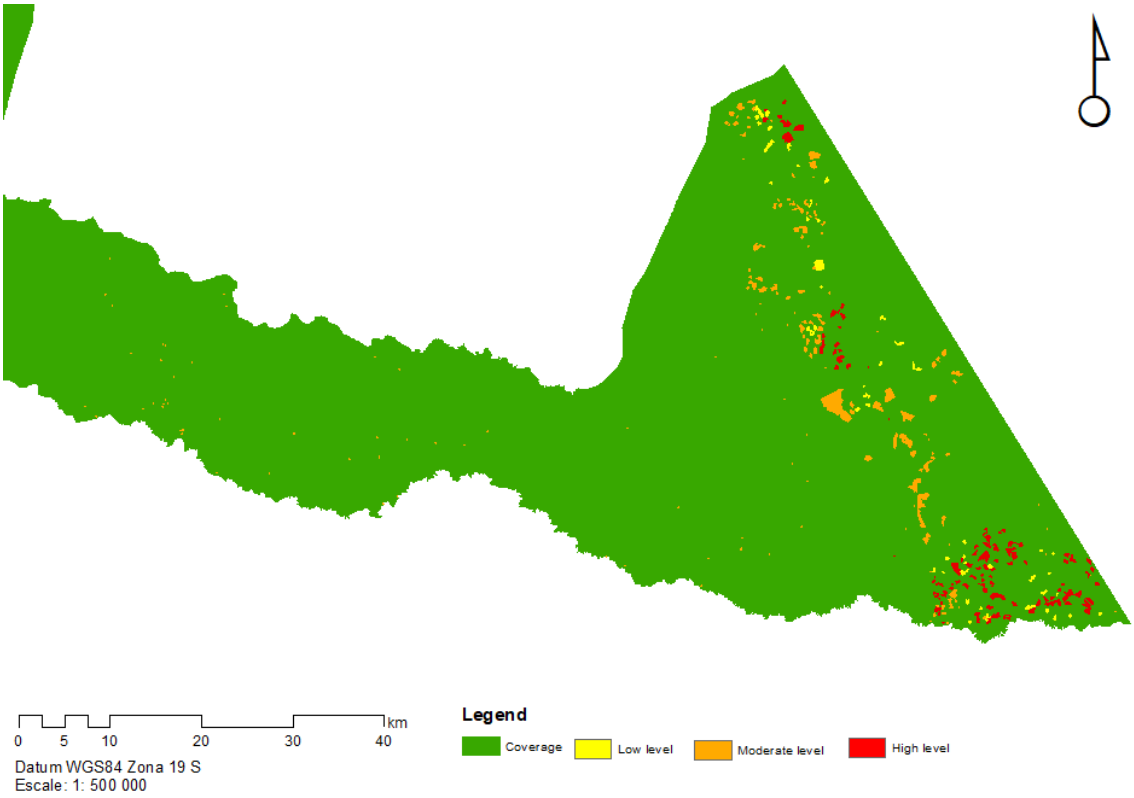

Figure S12. Burn severity using absolute, relative values from VH_2 pre- and post-fire 2020 backscatter data; Equation 2 and 6.

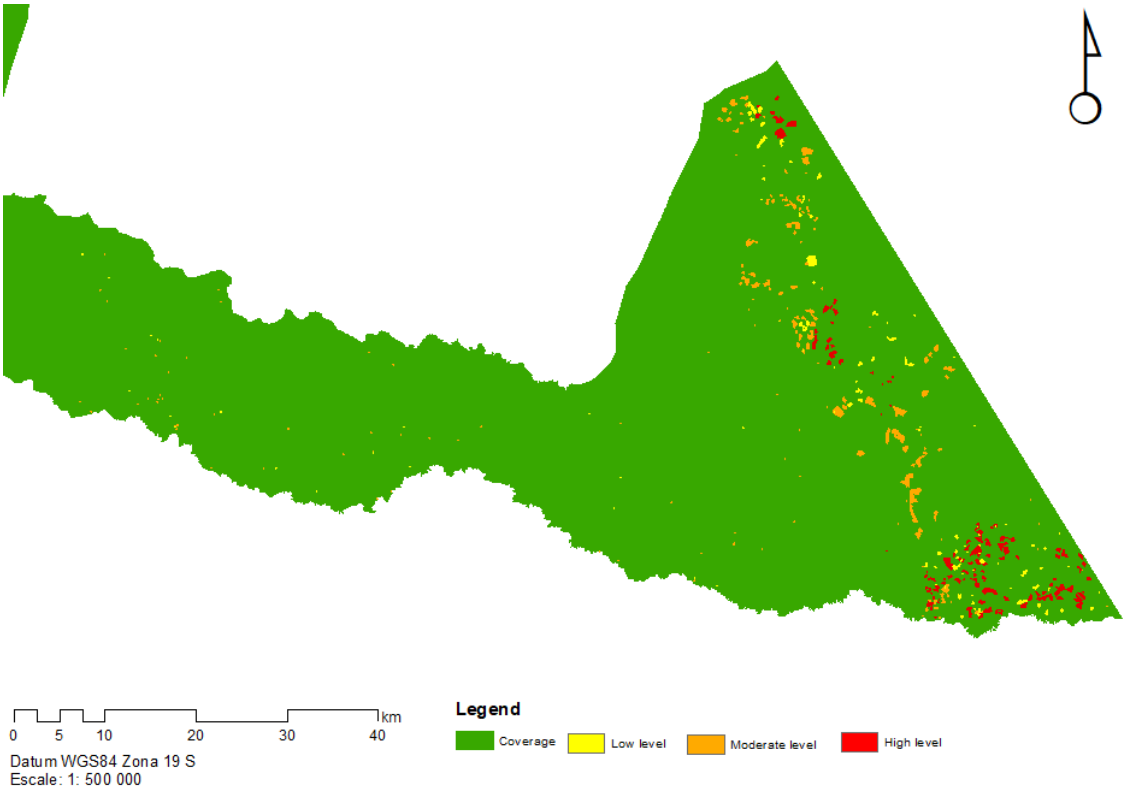

Figure S13. Burn severity using RADAR Burn Ratio (RBR) and RADAR Forest Degradation Index (RDFI) of pre- and post-fire 2020 VV and VH backscatter data; Equation 7, 8 and 9.